



Impacts of Baobab (*Adansonia digitata*) Powder on the Poly(Butylene Succinate) Polymer Degradability to Form an Eco-Friendly Filler-Based Composite

Musa Abubakar Tadda^{1,2}, Mostafa Gouda^{1,3*}, Xiaochang Lin¹, Abubakar Shitu^{1,2}, Hamza Sulayman Abdullahi^{4,5}, Songming Zhu¹, Xiaoli Li^{1*} and Dezhao Liu^{1*}

¹Key Laboratory of Equipment and Informatization in Environment Controlled Agriculture, Ministry of Agriculture and Rural Affairs, College of Biosystems Engineering and Food Science, Zhejiang University, Hangzhou, China, ²Department of Agricultural and Environmental Engineering, Faculty of Engineering, Bayero University, Kano, Nigeria, ³Department of Nutrition and Food Science, National Research Centre, Giza, Egypt, ⁴State Key Laboratory of CAD & CG, Zhejiang University, Hangzhou, China, ⁵Department of Mechanical Engineering, Faculty of Engineering, Bayero University, Kano, Nigeria

OPEN ACCESS

Edited by:

Manjeet Singh Goyat,
University of Petroleum and Energy
Studies, India

Reviewed by:

Zhanyong Wang,
Shenyang Agricultural University,
China
Amrita Hooda,
University of Petroleum and Energy
Studies, India

*Correspondence:

Mostafa Gouda
mostafa-gouda@zju.edu.cn
Xiaoli Li
Xiaolili@zju.edu.cn
Dezhao Liu
dezhaoliu@zju.edu.cn

Specialty section:

This article was submitted to
Polymeric and Composite Materials,
a section of the journal
Frontiers in Materials

Received: 01 September 2021

Accepted: 01 November 2021

Published: 30 November 2021

Citation:

Tadda MA, Gouda M, Lin X, Shitu A, Abdullahi HS, Zhu S, Li X and Liu D (2021) Impacts of Baobab (*Adansonia digitata*) Powder on the Poly(Butylene Succinate) Polymer Degradability to Form an Eco-Friendly Filler-Based Composite. *Front. Mater.* 8:768960. doi: 10.3389/fmats.2021.768960

Poly (butylene succinate) (PBS) is one of the most common biodegradable plastic polymers that has recently been used in the green environmental field. Enhancement of physicochemical characteristics of these polymers by using plant-based materials like Baobab (*Adansonia digitata*) will improve its industrial application. This study evaluated Baobab (*Adansonia digitata*) powder (BP) and PBS composites under various ratios (PBS/BP: 90/10, 80/20, 70/30, 60/40, and 50/50 wt%) for their thermo-mechanical and other physicochemical properties for the industrial application. The nanoscale morphological and elemental characterization were also measured by scanning electron microscope-dispersive X-ray spectroscopy (SEM-EDS). The results revealed that PBS/BP blends of 90/10 and 50/50 showed a significantly reduced melting temperature (T_m) up to 94°C ($p < 0.05$) compared to PBS (114°C). Also, the dynamic viscosity, storage modulus, and loss modulus showed a significant decrease with increasing the ratio of BP in PBS/BP composite, which confirmed faster degradation than the pure PBS. In conclusion, the novel PBS/BP biomaterial is recommended for use as a carbon source for denitrification processes, as an eco-friendly faster degradable natural filler-based polymer. Besides, they could be use in food packaging and biomedical industries.

Keywords: baobab (*Adansonia digitata*) powder, thermo-mechanical analysis, polymer degradability, poly(butylene succinate), dynamic viscosity, TGA and DSC analysis

INTRODUCTION

Using eco-friendly natural materials to decrease the environmental pollution exchange *via* emerging replacements of petroleum plastics with biodegradable materials has become one of the global key areas (Ramesh et al., 2017). The exponential growth in human population, urbanization, industrialization, exploration of natural resources, and pollutants' exchange *via* transboundary movements were identified as the main causes of environmental pollution (Ukaogo et al., 2020). Environmental pollution has remained a global challenge as multiple sources constantly contribute

immensely to change the environment's natural form. The environmental pollutions from different sources such as fuel and chemicals industries (including plastics) showed negative impacts on world marine production (Li et al., 2016; Barboza et al., 2018). Plastics industries, otherwise known as "super environmental deteriorators," have an estimated annual production of 360 million tons in 2018 and a forecast of attaining 500 million tons by 2025 (Lebreton and Andrady, 2019; Rafiqah et al., 2021). Some facts are that about 50% of the total plastics produced are single-use every year, out of which 500 billion single-use plastic bags are used globally: 700 plastic bags/year/person (Vuleta, 2021).

As commonly used filler-based for composites making, plastics (i.e., either from synthetic, semi-synthetic, or natural polymers) possessed some advantages such as high durability, corrosion-resistant, lightweight and cheap compared to other materials like metal and ceramic-based composites (Li et al., 2016; Bahl et al., 2020). These advantages are considered very useful, triggering their high acceptance rate globally. Although plastics may become brittle over time and break into smaller pieces, their degradation may take several decades, posing a serious threat to our environment (Barboza et al., 2018; Vuleta, 2021; Zhang et al., 2021). The common types of plastics that are widely used are one or a combination of the following polymers: polyethylene (PE), polybutylene succinate (PBS), polyvinyl chloride (PVC), polycaprolactone (PCL), polylactic acid (PLA), polyurethane (PUR), polyhydroxybutyrate (PHB), polypropiolactone (PPL), polystyrene (PS), polypropylene (PP), and polyethylene terephthalate (PET) (Barboza et al., 2018; Lebreton and Andrady, 2019; Bahl et al., 2020). Furthermore, to characterize these materials and their composites for suitability of application, several techniques were confirmed their suitability like X-ray diffraction (XRD), scanning electron microscopy-energy dispersive X-ray spectroscopy (SEM-EDS), thermogravimetric analysis (TGA), differential scanning calorimetry (DSC), Fourier-transform infrared spectroscopy (FTIR), and dynamic mechanical analysis (DMA). For instance, these techniques were reported by Mourdikoudis et al. (2018) as the most relevant characterization techniques for materials and their composites; hence, employed during this study.

Among the types of plastics previously mentioned, PBS has been reported as one of the most useful bio-based polyesters that its demand has kept rising over the years due to its excellent properties and promising sustainability (Rafiqah et al., 2021). As reported in previous literature, PBS has been applied in many areas for different purposes such as a source of carbon for denitrification (Liu et al., 2018; Qi et al., 2020), plastic bags (Xie et al., 2014), crops mulch cover (Su et al., 2019; Quattrosoldi et al., 2020); fishery materials, biomedical tools, tableware, etc. (Gigli et al., 2016; Rafiqah et al., 2021). However, despite the wide application of PBS in diverse areas, very limited studies paid attention to its faster degradation phenomena. Replacing the "hard-to-degrade" synthetic materials with the "easily-degradable" materials *via* blending with fiber and other materials was one of the best ways proposed by researchers to limit both macro-and-micro plastic's pollution (Yu et al., 2011; Barboza et al., 2018). Additionally, PBS was reported as the best

for maintaining its structural bonds during hot-melt mixings compared to the other biodegradable polymers (e.g., PLA and PCL) (Qu et al., 2019).

Baobab (*Adansonia digitata*) is a sub-Saharan African tree considered of high economic and cultural values as none of its parts (e.g., leaves, flowers, tubers, seeds, bark, fruit-pulp) is considered a waste, but a highly nutritious food with over 300 traditional application (Rahul et al., 2015; Ismail et al., 2019; Alba et al., 2020). Authorizing the use of "baobab fruit-pulp" by the European parliament in 2008 (EU: 2008/575/EC) as safe food for human consumption has triggered its commercial interest across the globe (Alba et al., 2020). Baobab powder (BP), obtained from the baobab fruit-pulp after the drying process, has many essential elements, both macro-and-micro nutrients like Sodium (Na), Magnesium (Mg), Phosphorus (P), Potassium (K), Iron (Fe), Manganese (Mn), Calcium (Ca) (Rahul et al., 2015). The BP also contained carbohydrates, vitamin C, protein, lipids, soluble and insoluble fibers (Rahul et al., 2015; Stadlmayr et al., 2020). In light of this, the highly underutilized fruit-pulp, BP as Kaimba et al. (2021) called it, could be blended with PBS and considered a filler-fibre. Also, Liang et al. (2010) reported significant improvements on PBS after blending with kenaf fibre (KF) through its high fiber content.

This paper aims to synthesis a novel degradable polymer composite from different concentrations of PBS and BP. Detailed analyses were conducted to determine the degradable nature of the newly developed PBS/BP composite by evaluating its thermal stability, storage ability, and potential as a substitute to pure PBS. Moreover, the newly developed material has undergone characterization through SEM-EDS, FTIR, and TGA-DTG, DSC, techniques to assess its thermal stability and morphological changes that may occur while in use. The XRD, viscosity, storage modulus, and loss modulus were also investigated.

MATERIALS AND METHODS

Materials

Extrusion grade biodegradable poly (butylene succinate) (PBS) was purchased from Dongguan Zhanyang Polymer Materials Co., Ltd. (Guangdong, China). The PBS's physical characteristics were: density, 1.26 g/cm³ at 25°C; molecular weight, 8.0 × 10⁴ g/mol; melting point, 115°C; melt flow rate 22 g/10 min; flexural strength, 40 MPa; and stress at break, 30 MPa. Also, the PBS was spheroidal in shape with a size of 4 × 3 × 2 mm (length × width × height) and porosity of 34.6%. Raw organic baobab (*Adansonia digitata*) powder (BP) was bought from MRM Nutrition Company (Oceanside, CA, United States). The BP powder was stored in an air-tight container and kept in the dark and dry condition until downstream application.

Synthesis of PBS/BP Blends

Before mixing, both PBS granules and BP were vacuum-dried for 24 h at 60 and 37°C, respectively. PBS/BPs at 90/10, 80/20, 70/30, 60/40, and 50/50 wt% were dry-mixed using a laboratory mixer (GM-300, Retsch GmbH, Germany) at 1,000 rpm. The various blends were then added into a batch mixer (CW Brabender,

United States) at 110–115°C using a rotor speed of 20 rpm. PBS/BP composites were then extruded using a double-screw extruder (HAAKE PolyLab OS, Thermo Fisher Scientific Inc., Germany) at 110–115°C. Hence, PBS/BP granules at 90/10, 80/20, 70/30, 60/40, and 50/50 wt% ratios were synthesized with the following physical characteristics: length \times diameter: 3 \times 2 mm (cylindrical shape); density, 1.18 g/cm³ at 25°C; porosity, 28.6%. Thin films were processed under compression from the PBS/BP blends at 130°C and used for viscosity, storage modulus, and loss modulus analyses.

Characterization of PBS/BP Blends and PBS

Chemical Structure Analysis by FTIR

The pure PBS and PBS/BP blends' chemical structure was characterized using FTIR instrument (Nicolet iS50FT-IR, Thermo Scientific, United States) to detect possible changes in major functional groups due to BP addition. The samples were scanned between a wavenumber range of 4,000–400 cm⁻¹.

X-ray Diffraction Measurement

XRD analysis was performed on the pure PBS and PBS/BP blends to determine the crystalline structure of the samples. After grinding the samples into powder, an X-ray diffractometer (XRD, D8 Advance Bruker diffractometer) was employed for the XRD analysis (40 kV, 40 mA).

Surface Morphology by SEM-EDS

The surface morphology and elemental composition of the pure PBS and PBS/BP blends were determined using GeminiSEM300 (Carl ZEISS Microscopy GmbH, Germany) equipped with a Bruker EDS detector which gives the SEM-EDS results at various magnifications. Before testing, the samples were placed in an ion sputter (MC1000, Hitachi, Japan) and coated with a thin layer of gold.

Thermogravimetric Analysis

TGA was conducted under nitrogen flow at 40 ml/min using TGA-Q500 (TA-Instruments, United States) to determine the behavioral degradation of the samples due to temperature increase. The test temperature was from 50 to 600°C at a heating rate of 10°C/min.

Differential Scanning Calorimetry for Thermal Behavior Analysis

The thermal behavior analysis was constructed using DSC-Q200 (TA-Instruments, United States). To eliminate previous thermal history, the samples were first heated at 150°C for 3 min, then cooled to -80°C at 10°C/min. Finally, the samples were reheated to 150°C at 10°C/min under a 50 ml/min nitrogen flow rate. About 6.50 mg of each sample was used with an accuracy of ± 0.10 mg.

Dynamic Mechanical Analysis

Dynamic mechanical analysis was conducted using DMA-Q800 (TA-Instruments, United States). Before conducting the DMA,

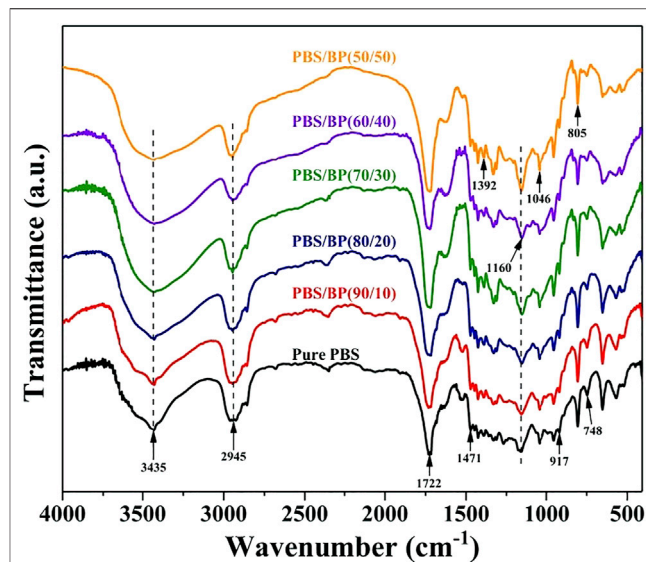


FIGURE 1 | FTIR spectra of the pure PBS and PBS/BP blends at varied ratios.

samples were prepared using a compression molder at 130°C. The samples were heated from 0 to 60°C at 3°C/min and 1 Hz frequency while recording the shear storage modulus and loss modulus changes.

Viscoelasticity Measurement

The viscosity of the pure PBS and PBS/BP blends was measured using a viscometer (HAAKE-RS6000, Thermo Scientific, Germany). Samples for the viscosity test were prepared using a compression molder at 130°C. The samples were then subjected to a shear rate range of 0.01–100 s⁻¹ at 130°C.

Mechanical Properties

A universal testing machine, Zwick/Roell Z020 (Zwick, Germany), was used to test the tensile properties of the pure PBS and the blends at a cross-head speed of 30 mm/min. At least five dumbbell-shaped samples were tested from each material with their average taken to get the mean value.

Data Analysis

For constructing all the spectra data for data analyses, average values \pm standard deviation (SD) were used. Analysis of variance (ANOVA) was used for all measurements, and $p \leq 0.05$ was considered statistically significant. Duncan, least significant differences (LSD), and Pearson tests have been calculated to measure the signification among the tested groups.

RESULTS AND DISCUSSION

Structural Analysis of the PBS/BP Blends and PBS

FTIR technique helps identify the chemical bonds and possible structural modifications that occurred due to blending PBS and

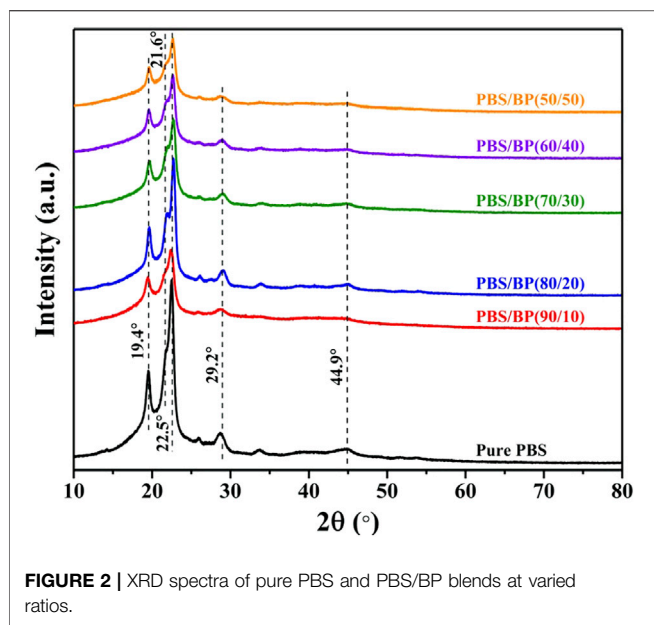


FIGURE 2 | XRD spectra of pure PBS and PBS/BP blends at varied ratios.

BP. As shown in **Figure 1**, it was observed from the FTIR spectra that the absorption bands assigned to functional groups showed a greater degree of similarity between the pure PBS and the PBS/BP blend at a higher wavenumber range ($4,000\text{--}1,750\text{ cm}^{-1}$), with more pronounced differences at lower wavenumber range ($1,750\text{--}400\text{ cm}^{-1}$). For both the pure PBS and PBS/BP blends, the absorption bands observed at $3,435$ and $2,945\text{ cm}^{-1}$ could attribute to the elongation vibration of the O–H and asymmetric stretching vibration of $-\text{CH}_2-$ groups, respectively (Zhu et al., 2015; Li et al., 2019).

Moreover, the absorption peaks at $1,722$, $1,471$, $1,392$, $1,160$, $1,046$, and 748 cm^{-1} were ascribed to the double bond of carbonyl ($\text{C}=\text{O}$), methyl of lignin's asymmetric bending ($-\text{CH}_3$), C–H deformation in cellulose and hemicellulose, stretching bond of ester ($-\text{C}-\text{O}-\text{C}-$), primary alcohol C–O bond, and aromatic rings of lignin, respectively (MonikaPal et al., 2018; Qi et al., 2020). Other important peaks obtained are 917 and 805 cm^{-1} attributed to C–OH bending in the carboxylic group and the cross-linking of the C–C bond, which affects the strength of ester linkages, as reported by MonikaPal et al., 2018. From these results, it was clear that the addition of BP had only slightly modified the pure PBS's composition while allowing its original functional chemical structure intact. Hence, the new PBS/BP blend would perform the functions of PBS at a greater significance, with other potentially added advantages envisaged.

Crystallization Behavior of the PBS/BP Blends and PBS

Figure 2 depicts the representative results of the XRD analysis of the PBS/BP blends and pure PBS. It was found that the PBS/BP blends were a replica of the semi-crystalline PBS as the two sharp peaks (19.4° and 22.5°) presented a decreasing nature of intensity due to an increase in BP's wt% in the blend. These two characteristics peaks obtained from the XRD spectrum, in

addition to 21.6 and 29.2 peaks, were similarly reported by Ye et al. (2017) after analyzing raw PBS and its blend with urea. Hence, the obtained crystalline structure results showed that the blends were just a numeral superposition and a physical mixture of PBS and BP with a reduced pure PBS crystallinity (Sadeghi et al., 2021) suggests faster degradation of the blends than pure PBS.

Mechanical Properties of the PBS/BP Blends and PBS

Table 1 shows the analyzed tensile properties of the pure PBS and the PBS/BP blends. It was observed from the results (**Table 1**) that pure PBS's Young modulus was $333 \pm 9.22\text{ MPa}$, which was consistent with the results reported for pure PBS in the previous literature (Delamarche et al., 2020; Jin et al., 2014). Furthermore, increases in Young's modulus values were recorded as the BP ratios were increased in the blends, as depicted in **Table 1**. This increase in Young's modulus values of pure PBS after blending with BP was similarly reported by Yang et al. (2010) after blending PBS with kenaf fibre. However, significant decreases ($p < 0.05$) were recorded for the yield strength and the maximum strain at break (i.e., fracture strain) as the BP ratios were increased, which were consistent with the results reported in the literature while increasing fibre ratio in PBS (Yang et al., 2010). Hence, these results implied that the higher the BP levels, the faster the degradability of the PBS and less energy required for elongation.

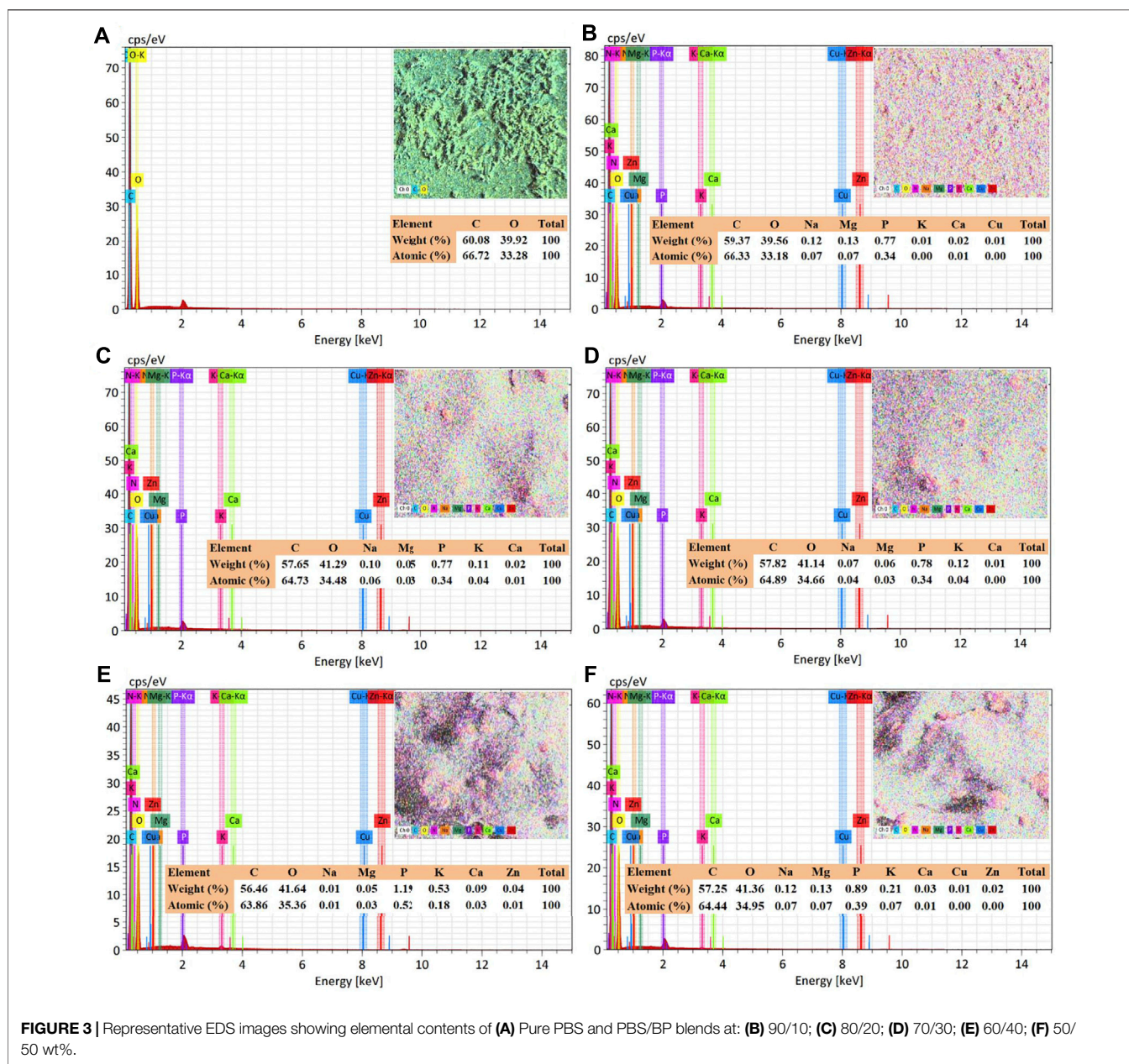
Morphological and Elemental Characterization of the PBS/BP Blends and PBS

Figure 3 showed detail of elemental contents of the PBS/BP blends using EDS, which revealed significant modification of pure PBS's original form mainly dominated by carbon ($\text{C} = 60.08\text{ wt}\%$) and oxygen ($\text{O} = 39.92\text{ wt}\%$), as depicted in **Figure 3A**. Meanwhile, **Figures 3B–F** represents the BP's level in the PBS/BP blends at 10, 20, 30, 40, and 50 wt%, respectively, with reduced molecular weight compared to pure PBS as it enhances faster degradation (Delamarche et al., 2020). Interestingly, the EDS results (**Figures 3B–F**) confirmed that the pure PBS was super enriched (after adding BP) by several essential elements, both macro-and-micro nutrients: Na, Mg, P, K, Ca, Cu, and Zn, at varied ratios (Rahul et al., 2015). These essential elements were reported by Singh (2021) to be solely responsible for biomolecule formation, metabolism, and co-factor of enzymes for protein structure stabilization in the cells. Additionally, these macro-and-micro nutrients were proved to be essential in supporting bacterial growth due to adequate nutrition supplementation (Li et al., 2019; Tadda et al., 2021). Besides, it was observed that higher BP content results in higher amounts of essential elements and less carbon and oxygen percent. Hence, faster degradation of PBS/BP will result in higher BP ratios, eventually releasing less carbon into the environment.

Figure 4 showed the SEM micrographs ($5,000\times$), depicting the morphology of PBS/BP blends and pure PBS to ascertain

TABLE 1 | Mechanical properties of pure PBS and PBS/BP blends.

Material	Young's modulus (MPa)	Yield strength (MPa)	Maximum strain at break (%)
Pure PBS	333 ± 9.22	24.0 ± 0.68	479.7 ± 23.20
PBS/BP(90/10)	502 ± 12.00	14.6 ± 0.88	3.4 ± 0.20
PBS/BP(80/20)	897 ± 4.61	17.7 ± 0.28	4.8 ± 0.50
PBS/BP(70/30)	1,050 ± 21.00	13.9 ± 0.50	3.2 ± 0.40
PBS/BP(60/40)	1,210 ± 19.10	12.4 ± 0.23	1.6 ± 0.10
PBS/BP(50/50)	1,220 ± 17.30	4.8 ± 0.91	0.5 ± 0.10



the levels at which their surface structure changes due to BP's addition. It was observed that pure PBS's surface morphology was dominated by coarser macro-voids which were unevenly

distributed (Figure 4A), compared with other micrographs from PBS/BP blends. Also, the micrographs (Figures 4B–F) showed asymmetric surface structures in which higher BP

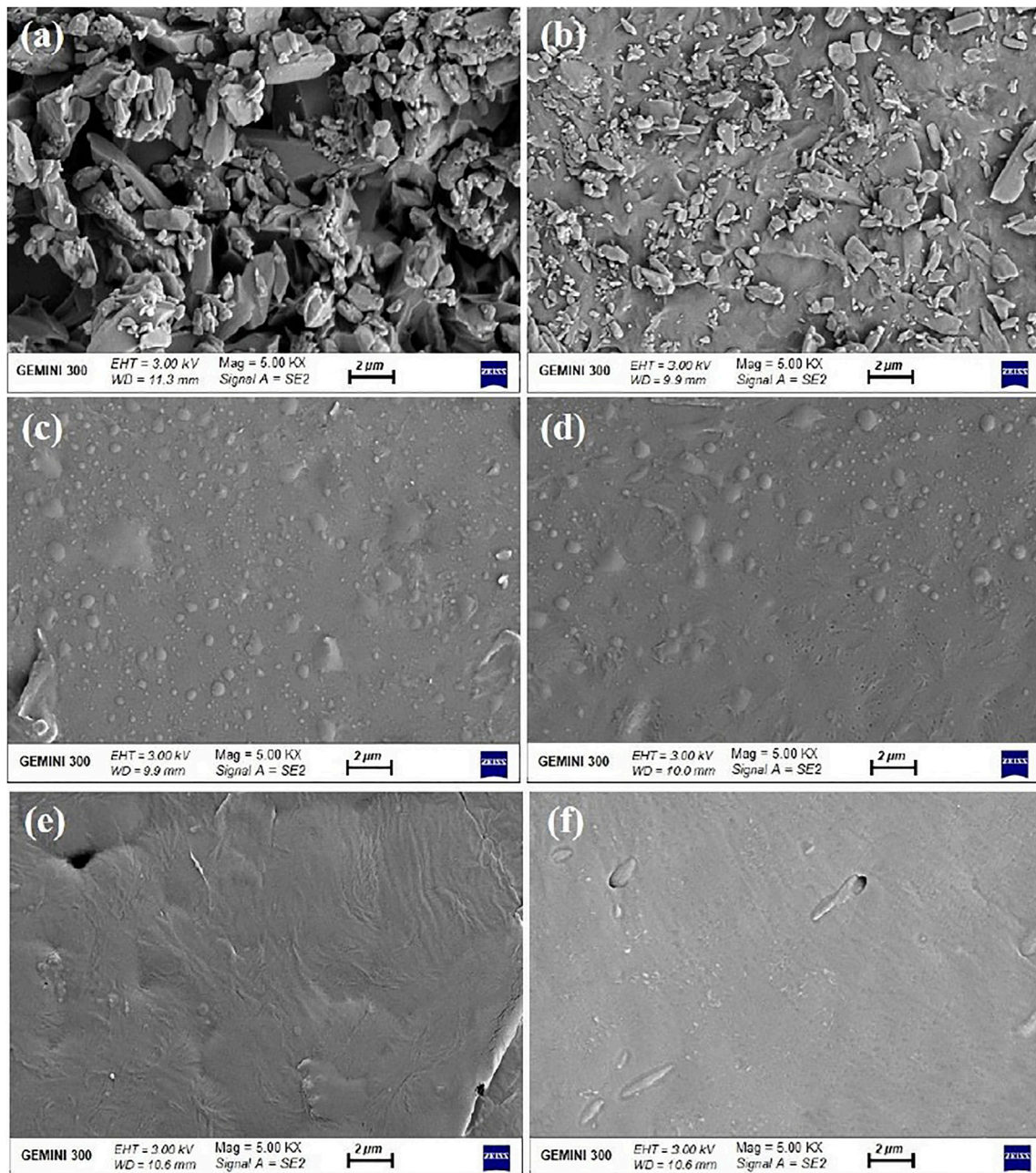


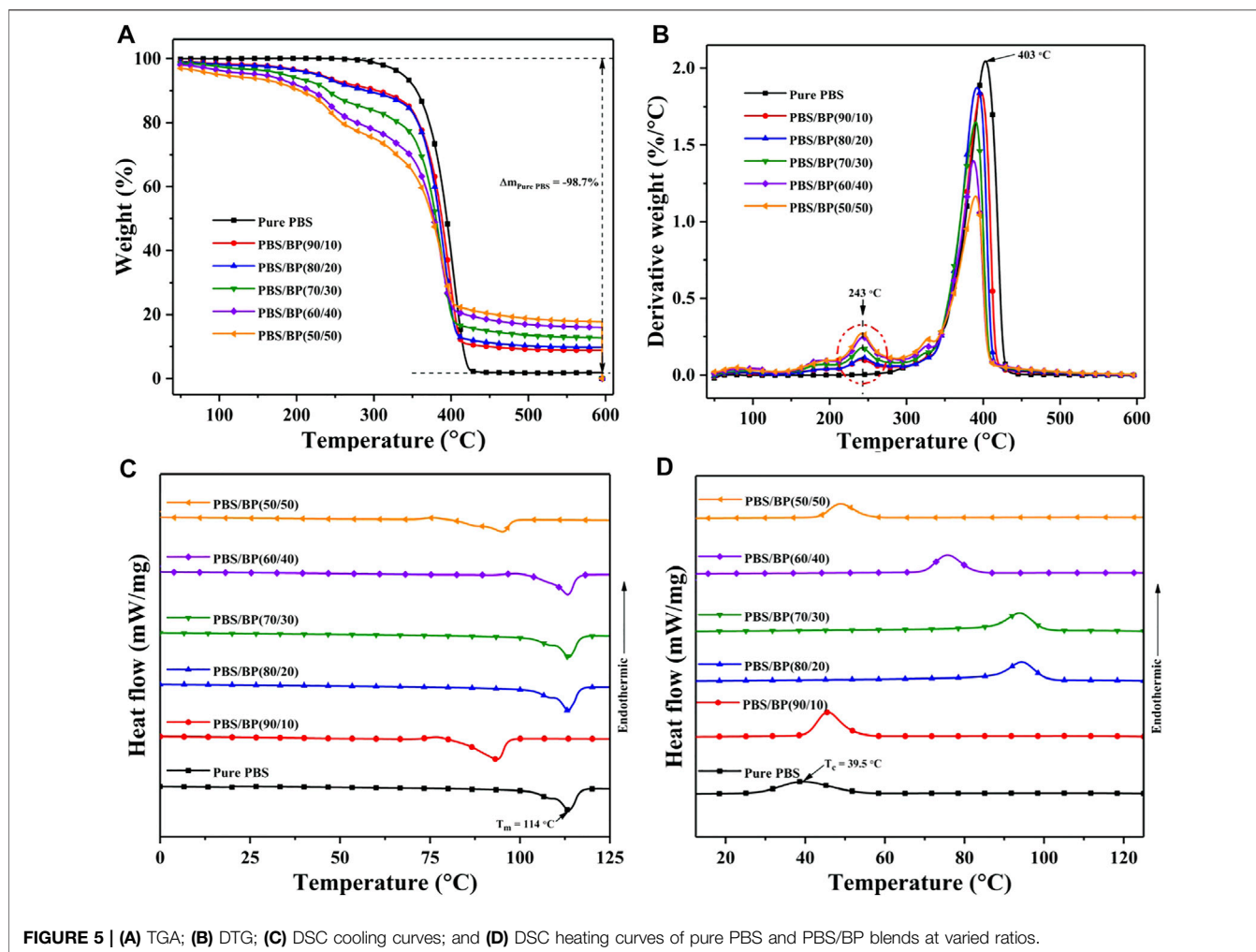
FIGURE 4 | SEM micrographs showing morphology of (A) Pure PBS; and PBS/BP blends at: (B) 90/10; (C) 80/20; (D) 70/30; (E) 60/40; (F) 50/50 wt%.

contents resulted in a reduction in the membrane porosity and cavity size due to the degradation of macro-voids of the pure PBS. When comparing the reduction in surface voids, the decreasing order of the PBS/BP blends' porosity due to BP addition was: 10 > 20 > 30 > 40 > 50 wt%. For instance, 50 wt% BP depicted in **Figure 4F** showed a smoother surface structure with fewer surface pores, which is more prone to degradation than 10 wt% BP presented in **Figure 4B**. Interestingly, our findings from the SEM micrographs were in total agreement with the results reported by Sadeghi et al. (2021), whereby a

higher amount of PBS (10 and 20 wt%) revealed an increase in both porosity and instability of pure PCL.

Thermo-Mechanical and Rheological Properties of the PBS/BP Blends and PBS

TGA and DSC curves which revealed thermal stability of the pure PBS and PBS/BP blends, were presented in **Figure 5**. It was observed from **Figure 5A** that the thermal degradation of pure PBS began at 285°C and achieved 98.7% weight loss at



425°C, which was consistent with a previous study (Hassan et al., 2013). For the PBS/BP blends, it was interesting to note that the degradation took place in three steps: 55–200°C; 200–330°C; and 330–410°C, with 50 wt% BP blend showing the fastest degradation (Figure 5A). This discovery confirmed that BP's addition had improved the degradation rate of the pure PBS in ascending order of BP's percent level in the blends, as clearly supported by the results from the derivative weight curve (DTG) in Figure 5B and that of SEM in Figures 4B–F. However, lower weight loss was observed from the blends than pure PBS due to higher ash content in the PBS/BP blends. This low weight loss was an indication that less carbon was released from the blends, which in practice will amount to reduced carbon pollution when the blends are used in place of pure PBS. Also, it is worth noting that from the DTG curves (Figure 5B), changes were observed in the PBS/BP blends' results from around 70–345°C, with the most significant change recorded at 243°C. Hence, better environmental management would emerge when the PBS/BP blends are used since their high ash content would add nutritional value to soil, ultimately leading to faster biodegradation and limiting carbon release to the environment.

Furthermore, DSC analysis results for both cooling and heating scans, were presented in Figures 5C,D, respectively. From the results, the melting temperature (T_m) of pure PBS was obtained as 114°C (Figure 5C), which was within the standard T_m for PBS (110–115°C) as reported in the previous studies (Dai and Qiu, 2016; Fenni et al., 2019; Delamarche et al., 2020). It was noted that PBS/BP blends of 90/10 and 50/50 showed a significantly reduced T_m of 94°C ($p < 0.05$) while other blends showing a T_m of a few degrees less of pure PBS (2–3°C) but with higher heat flow than the pure PBS (Figure 5C). However, for the crystallization temperature (T_c), which results due to cooling of the samples, significant variations were observed with fractionalized crystallization, as depicted in Figure 5D. This phenomenon of fractionated crystallization was a common behavior exhibited by polymer blends due to the heterogeneity of the blend materials (Fenni et al., 2019). Pure PBS had the lowest T_c of 39.5°C, and the lowest heat flow of 5.1 mW/mg, while PBS/BP blend at 90/10 recorded the highest peak (9.4 mW/mg) at T_c of 45.7°C (Figure 5D). In addition, it was also noted from the DSC results that the blends with the highest BP contents (40 and 50 wt%) had entered the

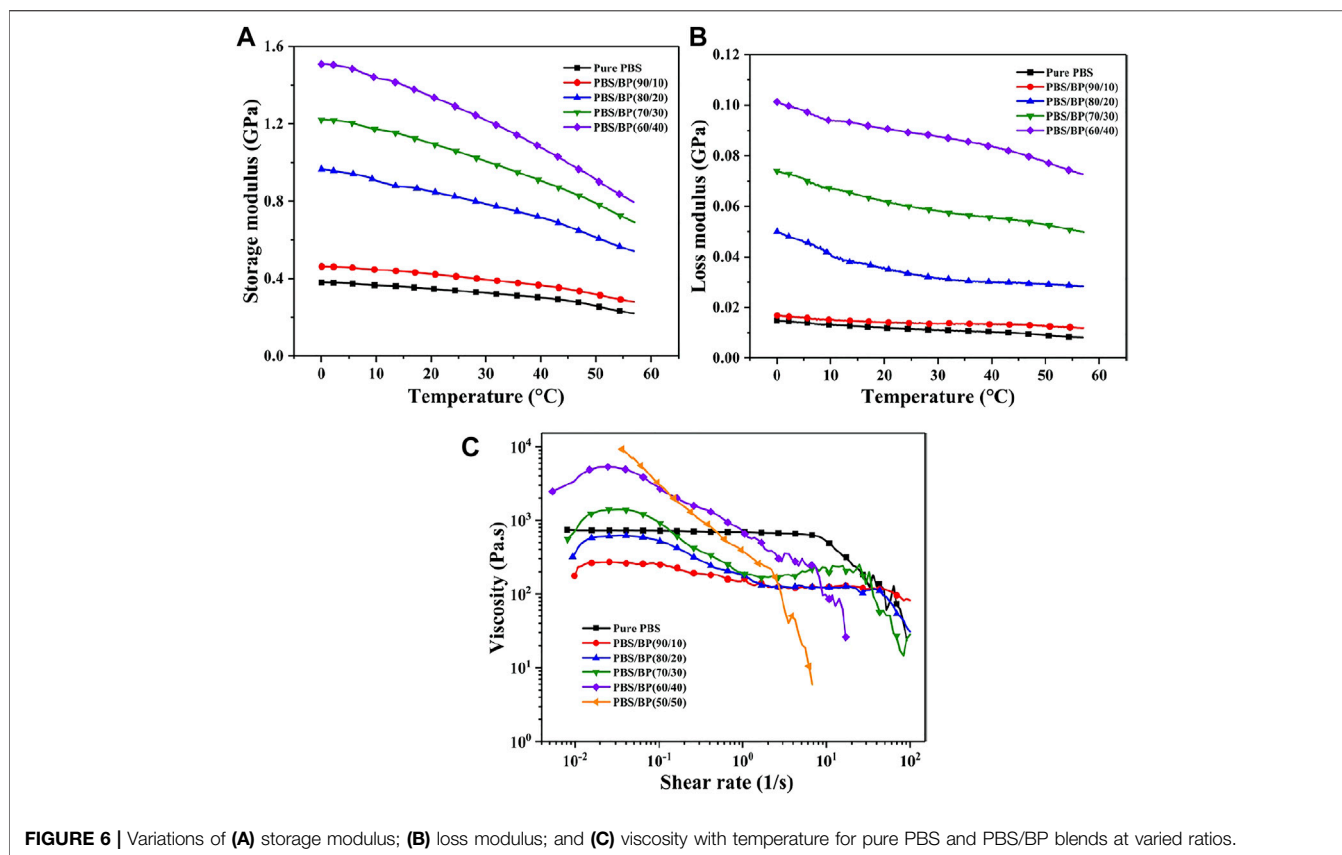


FIGURE 6 | Variations of (A) storage modulus; (B) loss modulus; and (C) viscosity with temperature for pure PBS and PBS/BP blends at varied ratios.

endothermic phase at 150°C with other samples showing a lag of 20°C during the endothermic phase change (130°C). Accordingly, these significant variations recorded for T_c have confirmed the changes in intermolecular interactions caused by blending BP with PBS, ultimately ensuring the blends' degradation at a faster rate.

The storage modulus (E') and loss modulus (E'') curves which depend on the variations of temperature, were presented in **Figures 6A,B**, respectively. It was observed that the E' curves displayed an obvious increasing tendency in ascending order of BP content's increase in the blends (**Figure 6A**), which was due to stress transfer from the pure PBS to the BP (Liang et al., 2010). Also, Liang et al. (2010) reported a result consistent with our finding whereby PBS's E' increased by more than 100% after blending with kenaf fiber (KF) at 90/10, 80/20, and 70/30 wt% (PBS/KF). It is worth noting that PBS/BP blends at 90/10 wt% showed the least increment of about 25%, while BP content of 20 wt% and above recorded more than 100% increase over the temperature ranges applied. For example, the storage modulus of pure PBS at 40°C was only 302 MPa but increased to 367, 714, 909, and 1,077 MPa for PBS/BP blends at 90/10, 80/20, 70/30, and 60/40, respectively. Such increases might be due to the increase in crystallinity of the PBS/BP blends as supported by the DSC curves explained earlier (**Figure 5D**).

More so, it was noted that E' values of both pure PBS and the PBS/BP blends keep decreasing with temperature increase

(**Figure 6A**), which was due to polymer matrix softening (Liang et al., 2010). It was observed that PBS/BP blend at 50/50 was too brittle to allow the test samples (size: 25 mm long, 5 mm wide, and 1 mm thick) to be carved out from the larger thin-film initially produced *via* compression molding. Therefore, this shows the unsuitability of using the 50/50 wt% combination to fabricate the targeted materials.

For the E'' values shown in **Figure 6B**, it was observed that both the pure PBS and PBS/BP blends exhibit the same manner displayed by E' results, whereby the PBS/BP blends recorded higher E'' values than pure PBS. However, the addition of 10 wt% BP had shown a slight increase in E'' values compared to higher increased E'' values recorded in ascending order, after adding 20 wt% BP and above. Therefore, the results of E' and E'' implied that further addition of BP, which simultaneously decreases the PBS wt%, decreases the blend's molecular mobility, hence reducing the intermolecular bond friction needed to overcome mechanical loss (Liang et al., 2010). Thus, the blends with higher BP wt% would degrade much faster than those with lower wt%, with however 20 to 30 wt% suggested as the best combination in the PBS/BP blend.

Figure 6C shows the variation of viscosity levels among the PBS/BP blends and pure PBS for varying temperatures. It was observed that pure PBS's viscosity decreased more rapidly after adding 10 and 20 wt% of BP. However, adding more than 20 wt% of BP had resulted in increased viscosity and irregular pattern of the viscosity curves, which might result from an

increase in rigidity of molecular chain and decrease in molecular weight of the blends (Qu et al., 2019). The reduction in viscosity level observed from this study due to an increase in BP and decrease in PBS agreed with a previous study that reported a reduction in viscosity due to a low amount of PBS (Sadeghi et al., 2021).

CONCLUSION

In the present study, biodegradable pure PBS was blended with BP at varied ratios (10, 20, 30, 40, and 50 wt% of BP) and synthesized PBS/BP blends with varied features. BP's addition leads to a decrease in crystallinity, molar mass, and thermal stability of the pure PBS filler polymer. Moreover, improvements in degradation rates were also observed, as evidenced by the SEM and thermomechanical tests conducted. Besides, EDS analysis revealed enrichment of the pure PBS with some essential elements (Na, Mg, P, K, Ca, Cu, and Zn), which were solely responsible for biomolecules formation, metabolism, and co-factor of enzymes for protein structure stabilization in the cells. Equally, these essential elements were very supportive of healthy and prosperous bacterial growth. Hence, the PBS/BP blends with improved degradability were recommended as a biodegradable carbon source for cleaner production of the advanced polymeric filler and composite formation. Also, the new PBS/BP composite could be applied in diverse areas where the pure PBS has been in operation, like disposable packaging plastic polymers and mulch cover for a cleaner environment.

REFERENCES

- Alba, K., Offiah, V., Laws, A. P., Falade, K. O., and Kontogiorgos, V. (2020). Baobab Polysaccharides from Fruits and Leaves. *Food Hydrocolloids* 106, 105874. doi:10.1016/j.foodhyd.2020.105874
- Bahl, S., Dolma, J., Jyot Singh, J., and Sehgal, S. (2021). Biodegradation of Plastics: A State of the Art Review. *Mater. Today Proc.* 39, 31–34. doi:10.1016/j.matpr.2020.06.096
- Barboza, L. G. A., Cózar, A., Gimenez, B. C. G., Barros, T. L., Kershaw, P. J., and Guilhermino, L. (2019). "Macroplastics Pollution in the marine Environment," in *World Seas: An Environmental Evaluation Volume III: Ecological Issues and Environmental Impacts*. Second Edn (Elsevier), 305–328. doi:10.1016/B978-0-12-805052-1.00019-X
- Dai, X., and Qiu, Z. (2016). Synthesis and Properties of Novel Biodegradable Poly(butylene Succinate-Co-Decamethylene Succinate) Copolyesters from Renewable Resources. *Polym. Degrad. Stab.* 134, 305–310. doi:10.1016/j.polymdegradstab.2016.11.004
- Delamarche, E., Mattlet, A., Livi, S., Gérard, J.-F., Bayard, R., and Massardier, V. (2020). Tailoring Biodegradability of Poly(Butylene Succinate)/Poly(Lactic Acid) Blends with a Deep Eutectic Solvent. *Front. Mater.* 7, 1–13. doi:10.3389/fmats.2020.00007
- Fenni, S. E., Wang, J., Haddaoui, N., Favis, B. D., Müller, A. J., and Cavallo, D. (2019). Crystallization and Self-Nucleation of PLA, PBS and PCL in Their Immiscible Binary and Ternary Blends. *Thermochim. Acta* 677, 117–130. doi:10.1016/j.tca.2019.03.015
- Gigli, M., Fabbri, M., Lotti, N., Gamberini, R., Rimini, B., and Munari, A. (2016). Poly(butylene Succinate)-Based Polyesters for Biomedical Applications: A Review. *Eur. Polym. J.* 75, 431–460. doi:10.1016/j.eurpolymj.2016.01.016

DATA AVAILABILITY STATEMENT

The original contributions presented in the study are included in the article/supplementary material, further inquiries can be directed to the corresponding authors.

AUTHOR CONTRIBUTIONS

MT: Conceptualization, Methodology, Investigation, Data curation and analysis, Writing—original draft, Writing—review and editing. MG: Conceptualization, Data analysis, Methodology, Writing—review and editing. XL: Writing—review and editing. AS: Writing—review and editing. HA: Data analysis, Writing—review and editing. SZ: Resources, Writing—review and editing. XL: Writing—review and editing, Funding acquisition, Resources. DL: Conceptualization, Methodology, Supervision, Funding acquisition, Writing—review and editing.

FUNDING

This research work was supported by the Key Research and Development Program of Zhejiang Province (No. 2021C02024), the National Natural Science Foundation of China (No.31802107; 32171889; and 32071895), and the National Key Research and Development Project (No. 2020YFD0900600; No. 2017YFD0701700). The graduate study was supported by the Two-High Scholarship at Zhejiang University, Hangzhou – China, and is well appreciated and acknowledged.

- Ismail, B. B., Guo, M., Pu, Y., Wang, W., Ye, X., and Liu, D. (2019). Valorisation of Baobab (*Adansonia Digitata*) Seeds by Ultrasound Assisted Extraction of Polyphenolics. Optimisation and Comparison with Conventional Methods. *Ultrason. Sonochem.* 52, 257–267. doi:10.1016/j.ultsonch.2018.11.023
- Jin, T.-x., Zhou, M., Hu, S.-d., Chen, F., Fu, Q., and Fu, Y. (2014). Effect of Molecular Weight on the Properties of Poly(butylene Succinate). *Chin. J. Polym. Sci.* 32, 953–960. doi:10.1007/s10118-014-1463-4
- Kaimba, G. K., Mithöfer, D., and Muendo, K. M. (2021). Commercialization of Underutilized Fruits: Baobab Pulp Supply Response to price and Non-price Incentives in Kenya. *Food Policy* 99, 101980. doi:10.1016/j.foodpol.2020.101980
- Lebreton, L., and Andrady, A. (2019). Future Scenarios of Global Plastic Waste Generation and Disposal. *Palgrave Commun.* 5, 1–11. doi:10.1057/s41599-018-0212-7
- Li, C., Liang, J., Lin, X., Xu, H., Tadda, M. A., Lan, L., et al. (2019). Fast Start-Up Strategies of MBBR for Mariculture Wastewater Treatment. *J. Environ. Manage.* 248, 109267. doi:10.1016/j.jenvman.2019.109267
- Li, W. C., Tse, H. F., and Fok, L. (2016). Plastic Waste in the marine Environment: A Review of Sources, Occurrence and Effects. *Sci. Total Environ.* 566–567, 333–349. doi:10.1016/j.scitotenv.2016.05.084
- Liang, Z., Pan, P., Zhu, B., Dong, T., and Inoue, Y. (2010). Mechanical and thermal Properties of Poly(butylene Succinate)/plant Fiber Biodegradable Composite. *J. Appl. Polym. Sci.* 115, 3559–3567. doi:10.1002/app.29848
- Liu, D., Li, J., Li, C., Deng, Y., Zhang, Z., Ye, Z., et al. (2018). Poly(butylene Succinate)/bamboo Powder Blends as Solid-phase Carbon Source and Biofilm Carrier for Denitrifying Biofilters Treating Wastewater from Recirculating Aquaculture System. *Sci. Rep.* 8, 3289. doi:10.1038/s41598-018-21702-5
- MonikaPal, A. K., Pal, A. K., Bhasney, S. M., Bhagabati, P., and Katiyar, V. (2018). Effect of Dicumyl Peroxide on a Poly(lactic Acid) (PLA)/Poly(butylene Succinate) (PBS)/Functionalized Chitosan-Based Nanobiocomposite for

- Packaging: A Reactive Extrusion Study. *ACS Omega* 3, 13298–13312. doi:10.1021/acsomega.8b00907
- Mourdikoudis, S., Pallares, R. M., and Thanh, N. T. K. (2018). Characterization Techniques for Nanoparticles: Comparison and Complementarity upon Studying Nanoparticle Properties. *Nanoscale* 10, 12871–12934. doi:10.1039/c8nr02278j
- Muhuo, Y., Wei, Y., Jiao, H., and Muhuo, Y. (2013). Dynamic Mechanical Properties and thermal Stability of Poly(lactic Acid) and Poly(butylene Succinate) Blends Composites. *Jfbi* 6, 85–94. doi:10.3993/jfbi03201308
- Qi, W., Taherzadeh, M. J., Ruan, Y., Deng, Y., Chen, J.-S., Lu, H.-F., et al. (2020). Denitrification Performance and Microbial Communities of Solid-phase Denitrifying Reactors Using Poly (Butylene Succinate)/bamboo Powder Composite. *Bioresour. Tech.* 305, 123033. doi:10.1016/j.biortech.2020.123033
- Qu, D., Sun, S., Gao, H., Bai, Y., and Tang, Y. (2019). Biodegradable Copolyester Poly(butylene-Co-Isosorbide Succinate) as Hot-Melt Adhesives. *RSC Adv.* 9, 11476–11483. doi:10.1039/C9RA01780A
- Quattrosoldi, S., Soccio, M., Gazzano, M., Lotti, N., and Munari, A. (2020). Fully Biobased, Elastomeric and Compostable Random Copolyesters of Poly(butylene Succinate) Containing Pripol 1009 Moieties: Structure-Property Relationship. *Polym. Degrad. Stab.* 178, 109189. doi:10.1016/j.polyimdegradstab.2020.109189
- Rafiqah, S. A., Khalina, A., Harmaen, A. S., Tawakkal, I. A., Zaman, K., Asim, M., et al. (2021). A Review on Properties and Application of Bio-Based Poly(Butylene Succinate). *Polymers* 13, 1436–1528. doi:10.3390/polym13091436
- Rahul, J., Jain, M. K., Singh, S. P., Kamal, R. K., AnuradhaNaz, A., Naz, A., et al. (2015). Adansonia Digitata L. (Baobab): A Review of Traditional Information and Taxonomic Description. *Asian Pac. J. Trop. Biomed.* 5, 79–84. doi:10.1016/S2221-1691(15)30174-X
- Ramesh, M., Palanikumar, K., and Reddy, K. H. (2017). Plant Fibre Based Bio-Composites: Sustainable and Renewable green Materials. *Renew. Sust. Energ. Rev.* 79, 558–584. doi:10.1016/j.rser.2017.05.094
- Sadeghi, A., Mousavi, S. M., Saljoughi, E., and Kiani, S. (2021). Biodegradable Membrane Based on Polycaprolactone/polybutylene Succinate: Characterization and Performance Evaluation in Wastewater Treatment. *J. Appl. Polym. Sci.* 138, 50332–50414. doi:10.1002/app.50332
- Singh, P. (2021). Nutritional and Physical Requirement for Bacterial Growth. Available at: <https://biokimicroki.com/nutritional-and-physical-requirement-for-bacterial-growth/>.
- Stadlmayr, B., Wanangwe, J., Waruhiu, C. G., Jamnadass, R., and Kehlenbeck, K. (2020). Nutritional Composition of Baobab (Adansonia Digitata L.) Fruit Pulp Sampled at Different Geographical Locations in Kenya. *J. Food Compos. Anal.* 94, 103617. doi:10.1016/j.jfca.2020.103617
- Su, S., Kopitzky, R., Tolga, S., and Kabasci, S. (2019). Polylactide (PLA) and its Blends with Poly(butylene Succinate) (PBS): A Brief Review. *Polymers* 11, 1193. doi:10.3390/polym11071193
- Sun, Y., Wu, L., Bu, Z., Li, B.-G., Li, N., and Dai, J. (2014). Synthesis and Thermomechanical and Rheological Properties of Biodegradable Long-Chain Branched Poly(butylene Succinate-Co-Butylene Terephthalate) Copolyesters. *Ind. Eng. Chem. Res.* 53, 10380–10386. doi:10.1021/ie501504b
- Tadda, M. A., Li, C., Gouda, M., Abomohra, A. E.-F., Shitu, A., Ahsan, A., et al. (2021). Enhancement of Nitrite/ammonia Removal from saline Recirculating Aquaculture Wastewater System Using Moving Bed Bioreactor. *J. Environ. Chem. Eng.* 9, 105947. doi:10.1016/j.jece.2021.105947
- Ukaogo, P. O., Ewuzie, U., and Onwuka, C. V. (2020). *Environmental Pollution: Causes, Effects, and the Remedies, Microorganisms for Sustainable Environment and Health*. Elsevier, 419–429. doi:10.1016/b978-0-12-819001-2.00021-8
- Vuleta, B. (2021). *51+ Disturbing Plastic Waste Statistics [2021 Update]*, 54/2910010. New YorkUSA: West 21st Street.
- Xie, L., Xu, H., Niu, B., Ji, X., Chen, J., Li, Z.-M., et al. (2014). Unprecedented Access to strong and Ductile Poly(lactic Acid) by Introducing *In Situ* Nanofibrillar Poly(butylene Succinate) for green Packaging. *Biomacromolecules* 15, 4054–4064. doi:10.1021/bm5010993
- Yang, Z., Peng, H., Wang, W., and Liu, T. (2010). Crystallization Behavior of Poly(ϵ -Caprolactone)/layered Double Hydroxide Nanocomposites. *J. Appl. Polym. Sci.* 116, 2658–2667. doi:10.1002/app.10.1002/app.31787
- Ye, H.-M., Chen, X.-T., Liu, P., Wu, S.-Y., Jiang, Z., Xiong, B., et al. (2017). Preparation of Poly(butylene Succinate) Crystals with Exceptionally High Melting Point and Crystallinity from its Inclusion Complex. *Macromolecules* 50, 5425–5433. doi:10.1021/acs.macromol.7b00656
- Yu, L., Ke, S., Zhang, Y., Shen, B., Zhang, A., and Huang, H. (2011). Dielectric Relaxations of High-K Poly(butylene Succinate) Based All-Organic Nanocomposite Films for Capacitor Applications. *J. Mater. Res.* 26, 2493–2502. doi:10.1557/jmr.2011.271
- Zhang, F., Zhao, Y., Wang, D., Yan, M., Zhang, J., Zhang, P., et al. (2021). Current Technologies for Plastic Waste Treatment: A Review. *J. Clean. Prod.* 282, 124523. doi:10.1016/j.jclepro.2020.124523
- Zhu, S.-M., Deng, Y.-L., Ruan, Y.-J., Guo, X.-S., Shi, M.-M., and Shen, J.-Z. (2015). Biological Denitrification Using Poly(butylene Succinate) as Carbon Source and Biofilm Carrier for Recirculating Aquaculture System Effluent Treatment. *Bioresour. Tech.* 192, 603–610. doi:10.1016/j.biortech.2015.06.021

Conflict of Interest: The authors declare that the research was conducted in the absence of any commercial or financial relationships that could be construed as a potential conflict of interest.

Publisher's Note: All claims expressed in this article are solely those of the authors and do not necessarily represent those of their affiliated organizations, or those of the publisher, the editors and the reviewers. Any product that may be evaluated in this article, or claim that may be made by its manufacturer, is not guaranteed or endorsed by the publisher.

Copyright © 2021 Tadda, Gouda, Lin, Shitu, Abdullahi, Zhu, Li and Liu. This is an open-access article distributed under the terms of the Creative Commons Attribution License (CC BY). The use, distribution or reproduction in other forums is permitted, provided the original author(s) and the copyright owner(s) are credited and that the original publication in this journal is cited, in accordance with accepted academic practice. No use, distribution or reproduction is permitted which does not comply with these terms.